UV–Curable L(-)–Borneol–Functionalized Antibacterial Hydrogels for Packaging of Fresh–Cut Banana and Cherry Tomato

Jizhong Yuan †, Yaohuang Jiang †, Mengle Liu, Peipei Wu, Guoxian Feng, Yanchun Yu *, Xiongfa Yang *

Posted Date: 2 April 2026

doi: 10.20944/preprints202604.0115.v1

Keywords: UV–curable hydrogel; antibacterial; L(-)–borneol; fresh–cut fruits and vegetables

 doi:10.20944/preprints202604.0115.v1

Article

UV–Curable L(-)–Borneol–Functionalized Antibacterial Hydrogels for Packaging of Fresh–Cut Banana and Cherry Tomato

Jizhong Yuan [1,†], Yaohuang Jiang [2,†], Mengle Liu [1], Peipei Wu [1], Guoxian Feng [1],Yanchun Yu [2,*] and Xiongfa Yang [1,*]

[1] Key Laboratory of Organosilicon Chemistry and Material Technology, Ministry of Education, Zhejiang Key Laboratory of Organosilicon Material Technology, College of Material, Chemistry and Chemical Engineering, Hangzhou Normal University, Hangzhou, 311121, Zhejiang, China

[2] College of Life and Environmental Sciences, Hangzhou Normal University, Zhejiang, 311121,China

* Correspondence: ycyu@hznu.edu.cn (Y.Y.); yangxiongfa@hznu.edu.cn (X.Y.)

† These authors contributed equally to this work.

Abstract

UV–curable L(-)–borneol–functionalized antibacterial hydrogels for packaging of fresh–cut banana and cherry tomato (UV–LBs) were designed from L(-)–Borneol–Functionalized polyurethane acrylate prepolymers (LB–PUAs) and thiol–functionalized PVA (PVA–SH) by UV initiated thiol–ene click reaction. UV–LBs exhibit good thermal stability with T_{d5} in the range of 225–240 °C, high mechanical performance with the tensile strength and the elongation at break in the range of 1.38–2.05 MPa and 44.4–68.6%, respectively. The antibacterial efficiency of UV–LBs against S. *aureus*, E. *coli*, and *M. albican* can reach 67.4%, 75.6% and 83.7%, respectively. The storage time of fresh–cut banana and cherry tomato packaged can be extended from 12 h to 30 h, 4 d to 5 d, respectively.

Keywords: UV–curable hydrogel; antibacterial; L(-)–borneol; fresh–cut fruits and vegetables

1. Introduction

Fruits and vegetables are necessary to human beings attributed to their merits of rich in vitamins, minerals and dietary fiber [1]. However, they are susceptible to spoilage due to microbial infections during the course of preservation and transportation [1–3]. As reported, about 42% fruits and vegetables were wasted during the course of preservation and transportation every year [1,4]. Recently, due to the increasing pace of modern life, the demand of convenient ready to–eat foods of fresh–cut fruits and vegetables is growing [5,6]. While, the cutting operations can induce mechanical injury, which will inevitably reduce the storage time of the fresh–cut fruits and vegetables for the bacterial inflection [7,8]. Obviously, developing packaging materials to prolong the preservation time of them are extremely urgent. The preservation methods for fruits and vegetables including packaging with coatings [9], adding antioxidant agents [10], and storing under the air conditioning [11] always encounter prominent drawbacks including high costs, requirement of specialized equipment and technology, and a great possibility of spoiling the taste or flavor [12]. So, develop antibacterial packaging materials to extend shelf life and reduce waste of fresh fruits and vegetables are urgently [1].

Antibacterial hydrogels, three–dimensional (3D) materials cross–linked by reversible covalent bonds or physical molecular interactions [13], possessing unique performance of soft, hydrophilicity and anti–microorganisms against bacteria, have gained increasing attention in food industry [14,15]. The antibacterial films prepared with polyvinyl alcohol (PVA) and nitrogen– doped carbon dots can delay the browning of fresh–cut apples [16]. Incorporated purple sweet potato anthocyanin and silver–nanoparticles into the chitosan/PVA, antibacterial composite films can extend the storage time

 doi:10.20944/preprints202604.0115.v1

of strawberries to 13 d at 4 ◦C [17]. By introducing Cu−tannic acid nanoparticles into a chitosan−gelatin matrix, the films exhibit killing efficiency of *E. coli* and *S. aureus* over 99%, and double the storage time of strawberries [18]. Antibacterial polysaccharide−based films prepared from sodium alginate and persimmon polysaccharides extraction incorporating of silver nanoparticles can keep the stability of pH and Vitamin C during the storage period [19]. However, these nanoparticle−contain antibacterial hydrogels have shortcomings of toxicity [20].

In response to these challenges, many hydrogels were designed avoid toxic nanoparticles. Pectin−based Schiff base functionalized films prepared from γ−aminobutyric acid and syringaldehyde displayed fairly high inhibition of E. *coli*, S. *aureus*, and B. *cinerea* over 24−48 h, and the papaya packaged can maintain the optimum firmness over 10 d [1]. Eco−friendly coatings fabricated from sodium carboxymethyl cellulose, lipopeptides and gelatin can extend the storage time of blueberries by 12.5% [21]. Packaging films developed from soy protein isolate, gelatin, rosemary−modified bentonite and glycerol for fresh lemon slices preservation can reduce weight loss to 37.89% and maintain freshness from 2 d to 4 d [22]. Antibacterial carrageenan−based films prepared with melanin extract can extend the storage time of strawberries for five days at 25± 2 ◦C [23]. PVA, a cost−effective, biodegradable and biocompatible polymer, is an ideal raw material to prepare hydrogels for food preservation [24]. A hydrogel film prepared from sodium carboxymethyl cellulose, PVA, tannic acid and ginkgo biloba leaf extract can prolong the storage time of strawberry for 7 d [25]. An antibacterial hydrogel prepared from soy hull nanocellulose, PVA, chitosan, and anthocyanin displayed an antibacterial efficiency of 90.59%, which can extend the storage time of salmon meat from 6 d to 14 d [26]. Gong et al. embedded a gallic acid−phycocyanin fiber mesh hydrogel into a PVA to produce a antibacterial fruit fresh−keeping film, which can prolong the storage time of grapes and blueberries to 13 d and 20 d at ambient temperature, respectively [27].

It is widely known that hydrogels prepared by physical molecular interactions often suffer from low mechanical properties and poor thermal stability [13,28]. To address these shortcomings, some hydrogels were cross−linked by Zn^{2+} or Fe^{2+} [29,30]. From another perspective, hydrogels were developed by covalent bonds using cross−linking agent, or functional molecule [31]. For example, Wang et al. used chitosan, PVA and ε−PL to fabricate a cross−linked multifunctional hydrogel, which can extend the storage time of chilled chicken to 8 d [32]. Similarly, organic cross−linking agents such as 1−ethyl−3−(3−dimethylaminopropyl) carbodiimide and N−hydroxysuccinimide were utilized to form stable amide covalent bonds so as to improve the mechanical property of hydrogels [33]. However, the network structure of these hydrogels will consist of either organic or inorganic compounds, which will limit the further application in food industry [34].

UV curing technology has drawn much attention due to the outstanding performance including eco−friendly, energy saving and high efficiency [14]. Polyurethanes (PUs) are among the most employed high−performance polymer materials in fields such as aerospace, automotive, electronics, deep−sea exploration due to their excellent mechanical properties, biocompatibility, chemical stability, and flexibility [35]. As reported, UV−curable pH−sensitive antibacterial hydrogels for monitoring the freshness of beef can be prepared from choline chloride and bromophenol red functionalized CS and thiol functionalized PU by UV−initiated thiol−ene click reaction [14]. The UV−curable hydrogels are with T_{d5} of 135.8−184.7 ◦C, the elongation at break of 117−525% and the tensile strength of 0.8−2.7 MPa. Antibacterial and pH−sensitive smart UV−curable hydrogels for shelf−life extension of chicken also can be developed from eugenol and bromocresol green functionalized polyurethane and thiol–modified chitosan [15]. These works revealed that UV curing technology can be adopted to develop hydrogels with good mechanical performance.

Borneol, a natural and lipophilic Chinese herbal medicine extracted from a variety of medicinal plants, is an ideal less toxic, environmentally friendly and broad−spectrum antibacterial material [36,37]. Zhao et al. designed natural antibacterial hydrogels via the Schiff base cross−linking of dialdehyde dextran grafted borneol and carboxymethyl chitosan. Thanks to the cooperation of hydrophilic borneol groups and positively charged ammonium ions of carboxymethyl chitosan, the hydrogels can constrict the E. *coli* and S. *aureus* growth in 24 h and demonstrate fairly good in vitro

 doi:10.20944/preprints202604.0115.v1

cytocompatibility [38]. Gao et al. developed antibacterial hydrogel with Yunnan Baiyao and Borneol, which demonstrated outstanding stretchability with elongation at break of ~1876%, and the inhibition zone of 8 mm against Staphylococcus aureus [39]. Hydrogels for infected burn wound healing were prepared with gallic acid functionalized PVA, 3−aminobenzeneboronic acid functionalized sodium alginate, Zn^{2+}, and chitosan−coated borneol nanoparticles [40]. Inspired by these interesting works, antibacterial UV−curable antibacterial hydrogels were designed from L(-)−Borneol−Functionalized polyurethane acrylate prepolymers (LB−PUAs) and thiol−functionalized PVA (PVA−SH) through UV initiated thiol−ene click reaction. The antibacterial performance, thermal stability and mechanical performance were investigated. The preservation investigation reveals that the hydrogels can obviously extend the storage time of fresh−cut banana and cherry tomato. It offers a potential strategy to develop antibacterial hydrogels for packaging fresh−cut fruits and vegetables with natural Chinese herbal medicine based polymers.

2. Materials and Methods

2.1. Materials and Reagents

L(-)−Borneol (98%), hydroxypropyl acrylate (HPA) and poly(ethylene glycol) with average molecular weight ~600 (PEG 600, A. R.) were bought from Macklin Biochemical Co., Ltd. (Shanghai, China). Trimethylolpropane (TMP, 98%) and poly(vinyl alcohol) (PVA, 1799) were from by Aladdin Biochemical Technology Co., Ltd. (Shanghai, China). Acetic acid glacial (A. R.) and 3−mercaptopropionic acid were purchased from Meryer Chemical Technology Co., Ltd. (Shanghai, China). 2−Hydroxy−2−methyl−1−phenylacetone (Irgacure−1173, 99.0%, AR), ditin butyl dilaurate (A. R.), absolute ethanol, concentrated sulfuric acid (98%) and isophorone diisocyanate (IPDI, 98%, mixture of isomers) were purchased from Sinopharm Chemical Reagent Co. Ltd, (Shanghai, China). *Staphylococcus aureus* (S. *aureus)*, *Escherichia coli* (ATCC 25922, E. *coli)*, Monilia *albican* (*M. albican*) and L929 cells were supplied by Testo Biochemical Co., Ltd. (Ningbo, China).

2.2. Synthesis of Thiol−Functionalized PVA (PVA−SH)

20.0 mL acetic acid glacial, 36.0 mL acetic anhydride, 0.40 mL concentrated sulfuric acid and 40.0 mL 3−mercaptopropionic acid were introduced into a 500−mL round−bottom flask in turn and mixed thoroughly. Then an aqueous solution of 4.00 g PVA in 100 mL deionized water was added into the mixture and the reaction was conducted at room temperature for 24 h. After that, 200 mL absolute ethanol was added and a white flocculation was produced. Subsequently, the white flocculation was obtained after centrifuged at 1500 r/min for 10 minutes and washed with absolute ethanol at least 3 times. Finally, the white solid of PVA−SH was put in a vacuum oven at 60 °C and dried overnight. The aqueous solution of PVA−SH was obtained by dissolving 7 g PVA−SH in 100 mL deionized water. PVA−SH and PVA were analyzed by FT−IR as shown by Figure S1. The absorption at 1056 cm^{-1} corresponds to the symmetric stretching vibration of C−O−C in PVA. The absorption at 1409 cm^{-1} is associated with the symmetrical bending of $-CH_2-$ while the absorption about 2983 cm^{-1} is attributed to the asymmetric and symmetric stretching vibrations of $-CH_2-$ [24]. The broad absorption peak around 3400 cm^{-1} is ascribed to the stretching vibrations of the−OH. There is a weak absorption about 2532 cm^{-1} ascribed to the characteristic vibration absorption of −SH in PVA−SH, respectively [14]. It reveals that the PVA−SH was successfully prepared.

2.3. Preparation of UV−Curable L(-)−Borneol−Functionalized Polyurethane Acrylate Prepolymers (LB−PUAs)

LB−PUAs were prepared according to the procedure presented at Figure S2. If the molar ratio of L(-)−borneol to HPA higher than 30:70, a large number of L(-)−borneol particles scattered in the LB−PUAs, which indicates that L(-)−borneol is in excess. Therefore, LB−PUAs were prepared by controlling the molar ratio of L(-)−borneol to HPA in the range of 0:100−30:70 as presented in Table

 doi:10.20944/preprints202604.0115.v1

1. For example, after 6.0 g PEG 600 (0.01 mol), 0.2683 g TMP (0.002 mol), 0.02 g Ditin butyl dilaurate and 30 mL acetone were mixed evenly at 40 °C, 7.2254 g IPDI (0.0325 mol) was added slowly for 2 h, the reaction was conducted at 60 °C for 2 h. Subsequently, a mixture of 4.0604 g HPA (0.0312 mol), 1.2031 g L(-)−borneol (0.0078 mol) were added at 40 °C followed the reaction was conducted at 60 °C for 4 h. Finally, a transparent sticky liquid of LB−PUA−20 was produced after the mixture was dried at 40 °C by vacuum for 4 h to remove acetone and the residual raw materials. The LB−PUAs were analyzed by FT−IR and ^{1}H NMR demonstrated by Figure S3 and Figure S4, respectively.

Table 1. Formula for preparation of LB−PUAs.

LB−PUAs	Molar ratio of L(-)−borneol to HPA	L(-)−borneol /mol	HPA /mol	PEG 600 /mol	TMP /mol	IPDI /mol
LB−PUA−0	0:100	0	0.0390			
LB−PUA−10	10:90	0.0039	0.0351			
LB−PUA−15	15:85	0.0059	0.0332			
LB−PUA−20	20:80	0.0078	0.0312	0.01	0.002	0.0325
LB−PUA−25	25:75	0.0098	0.0293			
LB−PUA−30	30:70	0.0117	0.0273			

2.4. Fabrication of UV−Curable Hydrogels (UV−LBs)

As presented in Figure S5, according to the molar ratio of acrylate groups to thiol groups of 1:1, the homogeneous mixtures of LB−PUAs, PVA−SH and 3 wt% Irgacure−1173 by the formula summarized in Table 2 were poured into the polytetrafluoroethylene molds. Then, the samples were cured by UV (365 nm,10.6 mW cm^{-2}) using a UV apparatus (ZB1000, Changzhou Zibo Electron Technology Co., Ltd., the distance of the slides to the UV light is 20 cm) for 20 s each face. The hydrogels prepared from LB−PUA−0, LB−PUA−10, LB−PUA−15, LB−PUA−20, LB−PUA−25 and LB−PUA−30 are named UV−LB−0, UV−LB−10, UV−LB−15, UV−LB−20, UV−LB−25 and UV−LB−30 in turn.

Table 2. Formula for preparation of UV−LBs.

UV−LBs	The categories and amount of LB−PUAs	The amount of PVA−SH
UV−LB−0	1 g LB−PUA−0	1.1925 g
UV−LB−10	1 g LB−PUA−10	1.0679 g
UV−LB−15	1 g LB−PUA−15	1.0060 g
UV−LB−20	1 g LB−PUA−20	0.9445 g
UV−LB−25	1 g LB−PUA−25	0.8833 g
UV−LB−30	1 g LB−PUA−30	0.8232 g

The amount of Irgacure−1173 is 3 wt% of the total mass of UV−LBs and LB−PUAs.

 doi:10.20944/preprints202604.0115.v1

2.5. Analytical Methods

2.5.1. Fourier–Transform Infrared (FT–IR) Spectroscopic Analysis

FT–IR analysis was carried out with a Nicolet 700 spectrometer (Nicolet Co., Ltd., American).

2.5.2. TGA (Thermogravimetric Analysis) Experiment

Thermal stability of UV–LBs was measured by TGA from room temperature to 800 ^{o}C with the heating rate of 10 ^{o}C min^{-1} in a N_2 atmosphere on a TG 209C apparatus (NETZSCH–Gerätebau GmbH, Selb, Germany).

2.5.3. Swelling Performance

The swelling behaviour of UV–LBs (Rectangular samples of 25.0 mm×25.0 mm×1 mm) was averaged after measured for 3 times and calculated using equation swelling rate% = $(W_t–W_0)/W_0×100\%$ [14,15]. Here W_0 and W_t are the mass of UV–LBs before and after swelled, respectively.

2.5.4. DMA Analysis

The mechanic properties of UV–LBs (50 mm×8 mm×1 mm) were studied by DMA using a DMA–Q800 instrument (TA Instruments, New Castle, USA) at 25 ^{o}C with a load of 0.1 N and tensile speed of 5 mm/min.

2.5.5. In Vitro Antibacterial Property Study

To study the antibacterial performance of UV–LBs, the coated plates and colony count method were conducted for 3 times each sample and averaged [14,15]. The sample without UV–LBs acted as control group (CK). Luria–Bertani (LB) was chosen to be medium for the antibacterial evaluation of *S. aureus* and *E. coli*, while YPDA (Yeast Peptone Dextrose Adenine) was chosen for the evaluation of *M. albican*. About 20 μL (10^5 CFU·mL^{-1}) bacterial suspensions were introduced into 20 mL media containing UV–LBs (Cylindrical samples, diameter is 10.0 mm and height is 1 mm). After *S. aureus* and *E. coli* were incubated at 37 °C or *M. albican* was incubated at 28 °C for 12 h in a shaking bed under 220 rpm, the antimicrobial activity was calculated according to the equation: Bactericidal ratio=$OD_{CK}–OD_{exp}/OD_{CK}–OD_{ini}$, here OD_{CK}, OD_{exp} and OD_{ini} are the values of optical density OD_{600} recorded on a microplate reader (Infinite 200 Pro, TECAN) for CK, experimental group and initial state correspondingly.

2.5.6. Bacterium and Fungi Morphology Study

According to the works reported [14,15], the bacterial morphology for S. *aureus*, E. *coli* and M.*albican* were studied using scanning electron microscope (SEM, SEMS–3000N, Japan, Hitachi Co., Ltd.). Typically, after centrifuged, washed, fixed with 2.5% glutaraldehyde and kept for 24 h at 4 °C, the bacterial cells on the UV–LBs were washed with PBS and fixed with 1% osmium acid for about 1 h. Later, the bacterial cells were dehydrated with a graded ethanol solution and isoamyl acetate in turn. After the UV–LBs were dried completely and coated with gold–palladium, the bacterial morphology was studied.

2.5.7. In Vitro Cytotoxicity Assay

The in vitro cytotoxicity was assessed by the optical density of OD_{450} value and the relative cell viability against L929 cells according to reference 15. The cell viability was obtained according to *Cell viability* (%)=$(OD_s–OD_b)/(OD_n–OD_b)$×100%, here OD_s, OD_b and OD_n represent the absorbance of the sample group, blank group, and negative control group.

 doi:10.20944/preprints202604.0115.v1

2.5.8. Packaging Investigation of Fresh−Cut Banana and Cherry Tomato

The packaging investigation of fresh−cut banana and cherry tomato was conducted as shown in Figure S6. Slices of fresh−cut cherry tomato and banana were put onto each film of hydrogel and then packaged. To make a comparison, the fresh−cut banana and cherry tomato slices samples exposed to air directly were named CK. After a period of time, the slices of banana and cherry tomato were taken out carefully and taken photos with an iPhone 11 pro to record their status by Jizhong Yuan.

2.5.9. Statistical Analysis

The experiment for the antibacterial performance were conducted for 3 times. A minimum of 3 experiments of Excel (Microsoft, Redmond, VA, USA) was utilized to evaluate the means and standard deviations.

3. Results and Discussion

3.1. FT–IR Analysis

The FT−IR analysis of LB−PUA−30 and UV−LB−30 was conducted as exhibited in Figure S7. The absorption at 3458–3210 cm^{-1} is assigned to the stretching vibrations of –OH and $–NH_2$. The absorption at 2956–2870 cm^{-1} is ascribed to the stretching vibration of –C–H. The absorption at 1699–1703 cm^{-1} and 1418–1420 cm^{-1} are attributed to the stretching vibration of –C=O and deformation vibration of $–CH_3$ in $–NHCOCH_3$ groups, respectively. There is a weak characteristic absorption of –C=C– in acrylate groups at 1620 cm^{-1} in the spectrum of LB−PUA−30 while there is no characteristic absorption of –C=C– in acrylate groups in FT−IR spectrum of UV−LB−30, which indicates that UV−LBs can be cured almost completely for 20 s each face.

3.2. Thermal Stability Investigation of UV−LBs

The antibacterial hydrogels with good thermal stability have potential application in packaging the food cooked at a relative high temperature or medical materials require high−temperature sterilization. So, TGA analysis was adopted to investigate the thermal stability of UV−LBs. As presented in Figure S8, the initiate thermal decomposition temperature (T_{d5}) of UV−LBs is in the range of 225−240 °C, which decreased with the increment of the molar ratio of L(-)−borneol to HPA from 30:70 to 0:100. The decline of T_{d5} is due to the poor thermal stability of L(-)− borneol groups [41]. Above all, the hydrogels prepared possess good thermal stability.

3.3. Swelling Behavior of UV−LBs

Swelling rate is a significant impact to evaluate the water absorption ability and stability of hydrogels, which is essential for the practical applications of food packaging, wound healing and wearable electronics [14,42,43]. Therefore, the swelling rate of UV−LBs prepared with different molar rate of L(-)−borneol to HPA was studied as shown in Figure 1. It can be seen that the swelling equilibrium was established after the UV−LBs samples were immersed in deionized water for 10 h and the swelling rate is in order of UV−LB−30<UV−LB−25<UV−LB−20<UV−LB−15< UV−LB−10<UV−LB−0. When the molar ratio of L(-)−borneol to HPA increased from 0:100 to 30:70, the swelling rate of UV−LBs reduced from 80% to 32% correspondingly, which means the water absorption ability decreased with the increment of the amount of covalent grafted LB groups L(-)−borneol.

 doi:10.20944/preprints202604.0115.v1

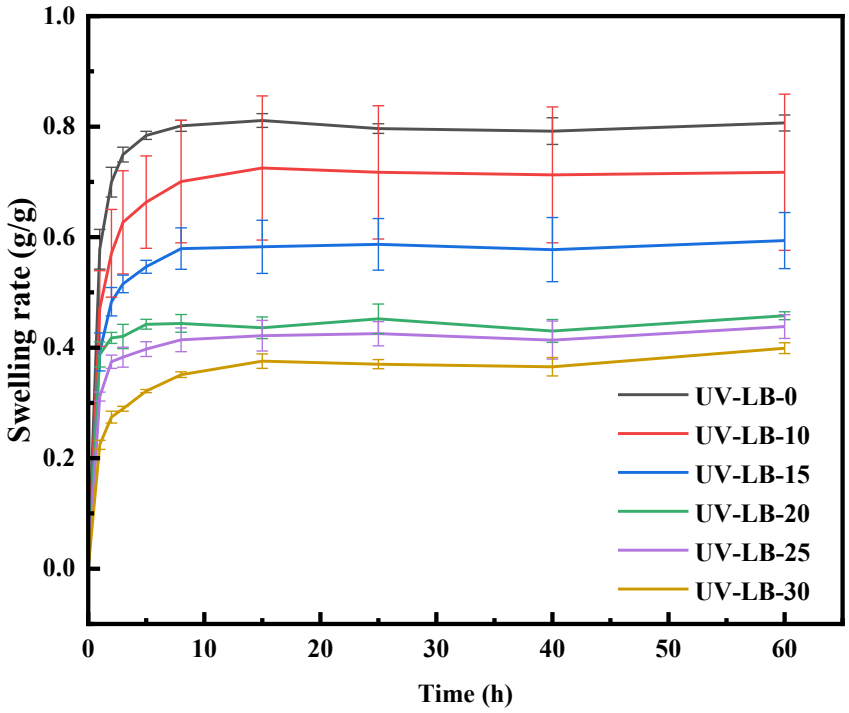

Figure 1. Variation of swelling rate with time.

3.4. DMA Analysis of UV−LBs

The mechanical performance of UV−LBs was evaluated by DMA analysis shown in Figure S9. The tensile strength and elongation at break of UV−LBs are in the range of 1.38−2.05 MPa and 44.4−68.6%, respectively. As we know, one of the efficient chemical modification strategies is incorporation of rigid chemical groups to improve the mechanical performance of materials [44,45]. Just agree with them, when the molar ratio of L(-)−borneol to HPA is 15:85, the highest tensile strength of UV−LBs (2.05 MPa) achieved by balancing the flexible units and the rigid units [46]. Making a comparison with the non−ionic UV−curable hydrogel developed by Liu with a tensile strength of 0.1−0.43 MPa, it is convinced that the UV−LBs are with a higher tensile strength [46].

3.5. Antibacterial Property of UV−LBs

3.5.1. Antibacterial Property Evaluated with the Coated Plates and Colony Count Method

The antibacterial property of UV−LBs was studied by the coated plates and colony count method as shown in Figure 2. From Figure 2a, it can be concluded that the antibacterial efficiency against *E. coli* increased with the increasing of the molar ratio of L(-)−borneol to HPA because the number of bacterial colonies turned less and less correspondingly. It reveals that a higher amount of L(-)−borneol groups in UV−LBs will achieve a higher antibacterial efficiency. The antibacterial efficiency against *S. aureus, E. coli* and *M. albicans* was compared as shown in Figure 2b. By the coated plates and colony count method, the antibacterial efficiency against *S. aureus, E. coli* and *M. albicans* was 67.4%, 75.6% and 83.7%, respectively. So, the UV−LBs exhibit a quite high antibacterial efficiency, especially for *M. albicans*.

 doi:10.20944/preprints202604.0115.v1

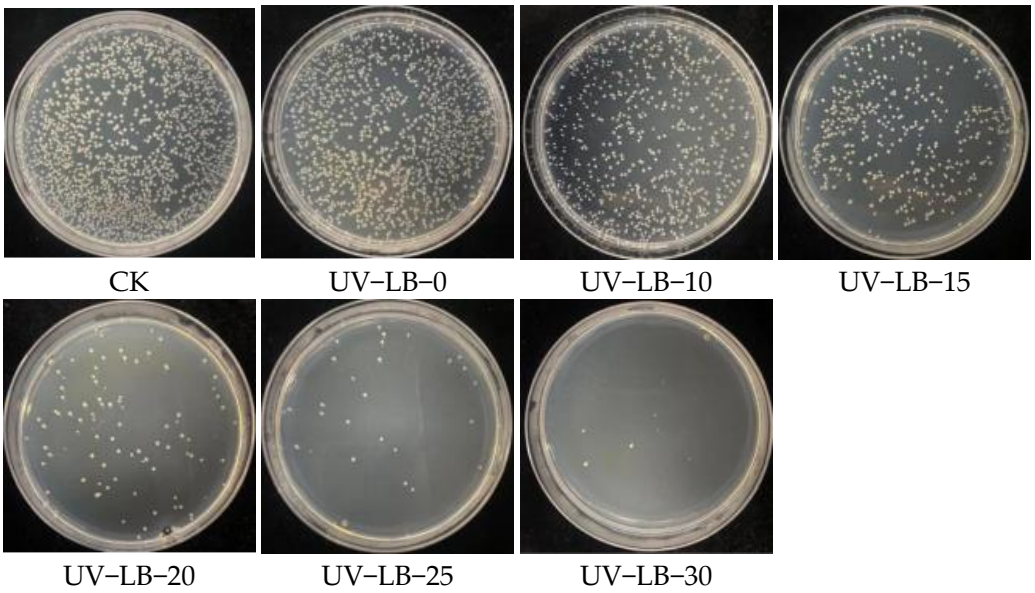

(a) Antibacterial performance of different UV−LBs against *E. coli*

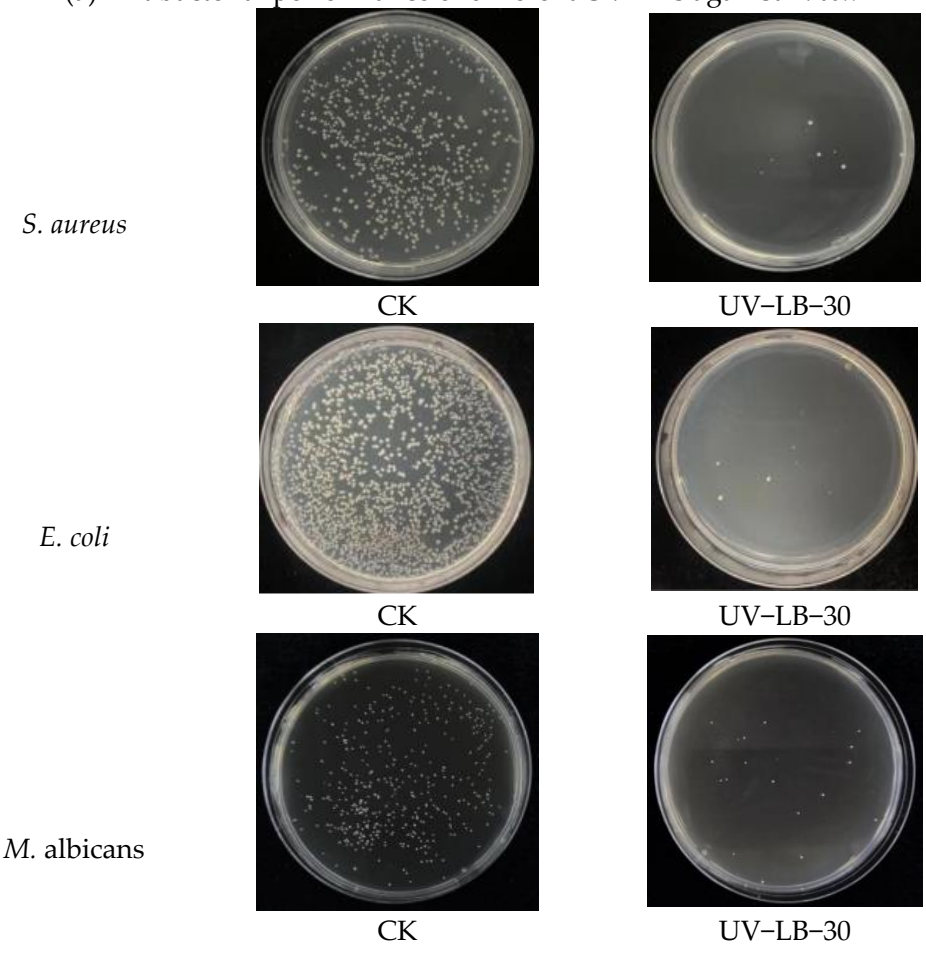

(b) Antibacterial performance of UV−LB−30 against *S. aureus*, *E. coli* and *M.* albicans

Figure 2. Antibacterial property evaluated with the coated plates and colony count method.

3.5.2. OD_{600} Evaluation of UV−LBs Using Co−Culturing Method

To evaluate the antibacterial efficiency with co−culturing method, the OD_{600} value was measured as shown in Figure 3. Under the same condition, a lower OD_{600} value usually means a higher antibacterial efficiency [14,15]. The OD_{600} values of UV−LBs were in sequence of UV−LB−30<UV−LB−25<UV−LB−20<UV−LB−15<UV−LB−10<UV−LB−0<CK, which implies the antibacterial efficiency of UV−LBs against *S. aureus*, *E. coli* and *M. albican* in order of

 doi:10.20944/preprints202604.0115.v1

CK<UV−LB−0<UV−LB−10< UV−LB−15<UV−LB−20<UV−LB−25<UV−LB−30. So, a higher molar ratio of L(-)−borneol to HPA will achieve a higher antibacterial efficiency thanks to a higher content of antibacterial functionalized groups of L(-)−borneol. Hence, the UV−LB−30 exhibited the highest antibacterial efficiency of 67.4% after 7 h against S. *aureus*, 75.6% after 8 h against E. *coli*, and 83.7% after 13 h against M. *albicans*.

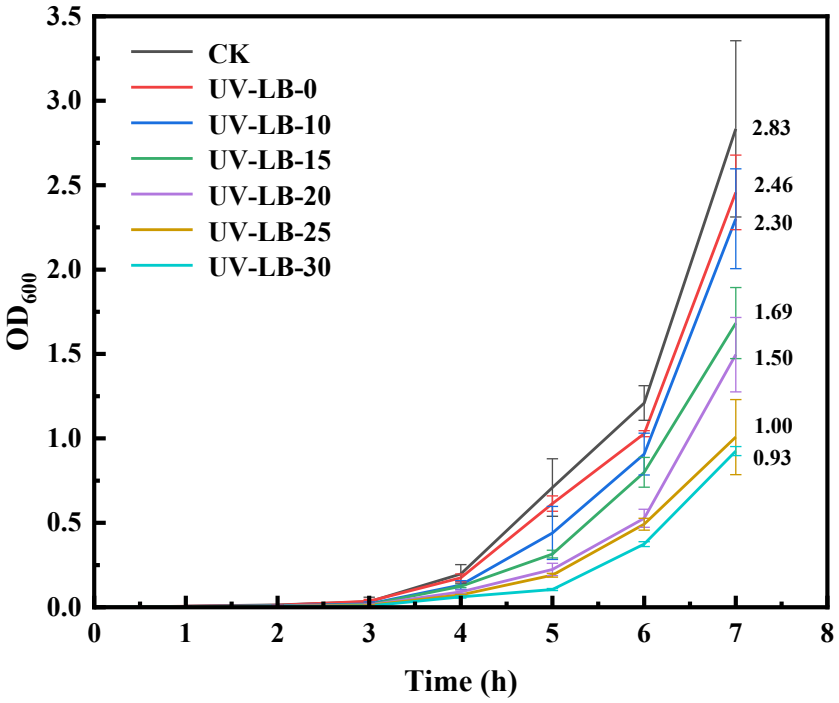

(a)S.aureus

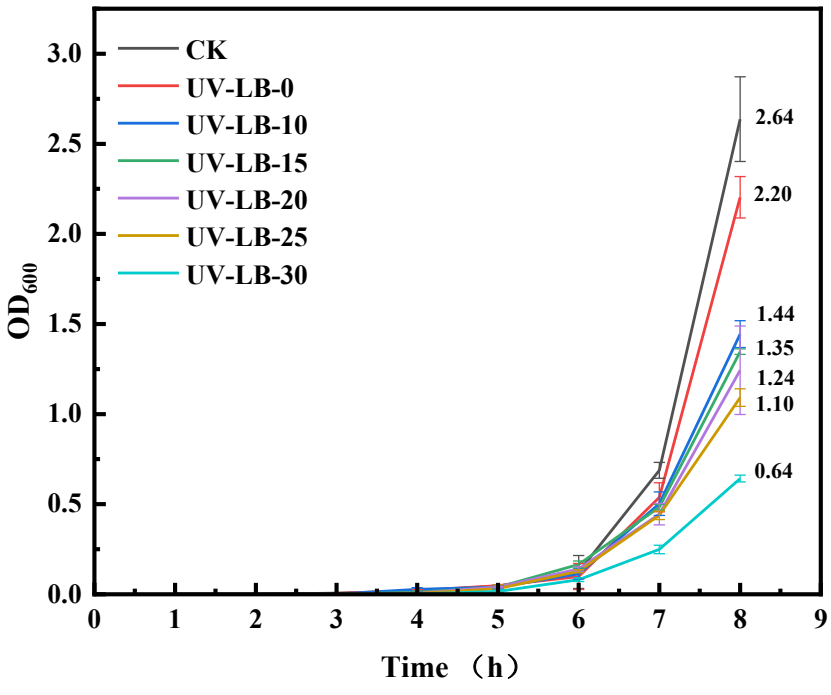

(b)E. coli

 doi:10.20944/preprints202604.0115.v1

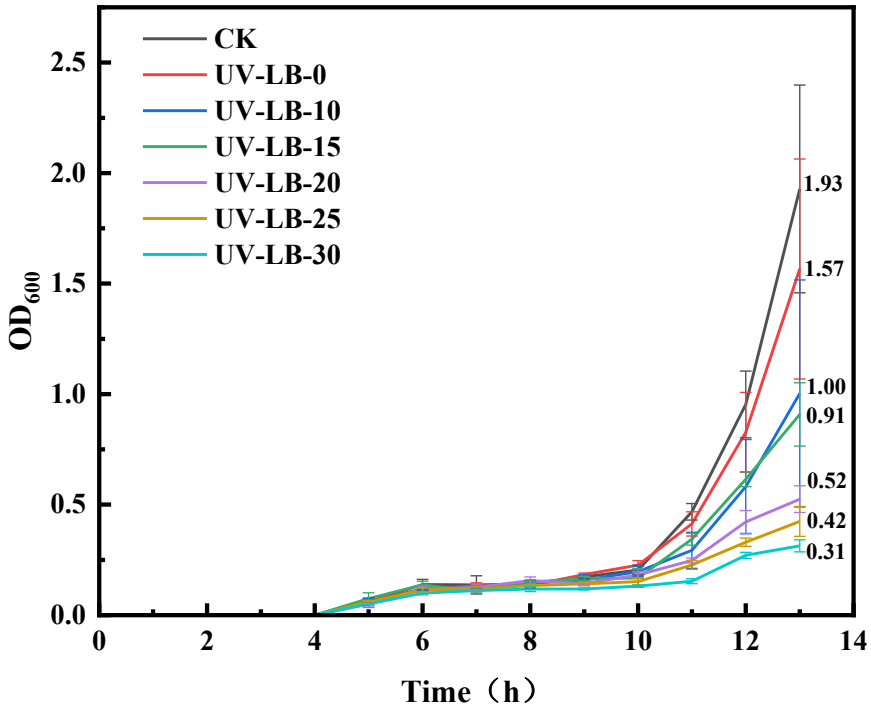

(c)M. albican

Figure 3. OD_{600} value measured with co−culturing method.

3.5.3. Bacterium and Fungi Morphology Study

The morphology of S. *aureus*, E. *coli* and M. *albican* co−cultured with UV−LB−30 was investigated by SEM analysis shown in Figure 4. Clearly, the morphology of S. *aureus*, E. *coli* and M. *albican* cells after 24 h co−cultivation was either deformed or cracked, which means the bacterium and fungi were killed by attachment of UV−LBs.

S. *aureus*

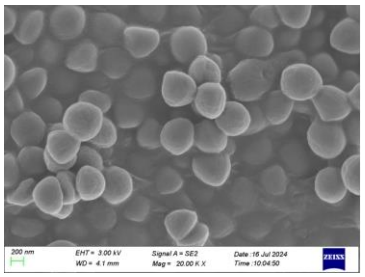

Before co−cultured

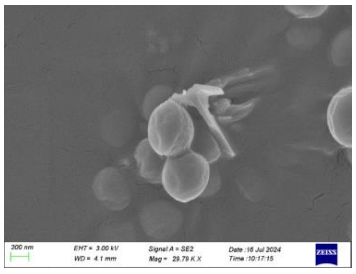

After co−cultured

E. *coli*

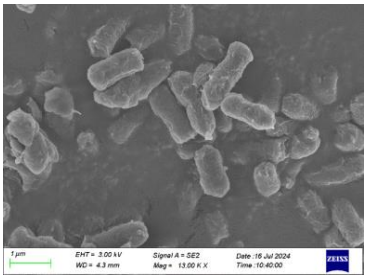

Before co−cultured

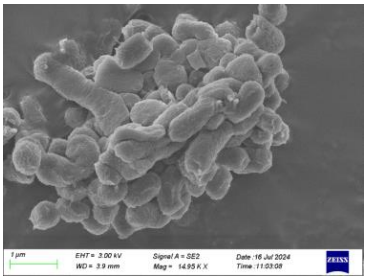

After co−cultured

 doi:10.20944/preprints202604.0115.v1

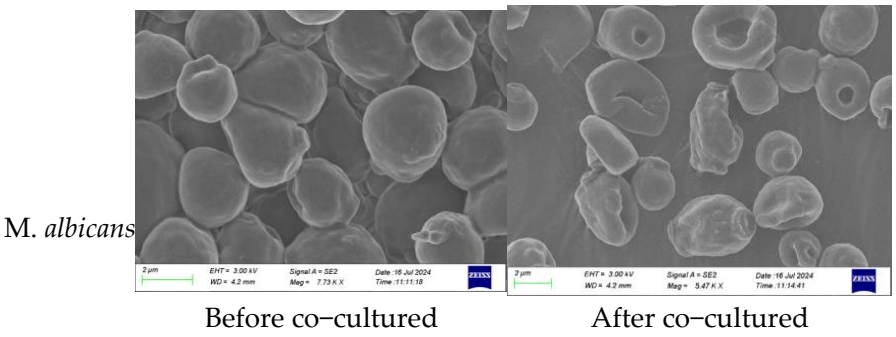

Figure 4. Morphology of *S. aureus, E. coli* and *M. albican* before and after co−cultured.

3.6. Cytotoxicity Assay

OD_{450} values and cell viability of UV−LBs against L929 cells was studied. As presented in Figure 5a, after 5 d, the OD_{450} values of UV−LBs grafted LB groups were in the range of 0.35−0.49, which were lower than that of UV−EB−0 (NC, about 0.56). As shown by Figure 5b, the cell viability of UV−LBs grafted LB groups was in the range of 60%−80%, which suggested the UV−LBs grafted LB groups were with fairly low toxicity against L929 cells. Though the toxicity increased with the increasing of LB groups grafted, it is lower than Borneol, a natural less toxic, environmentally friendly and broad−spectrum antibacterial material [36,37].

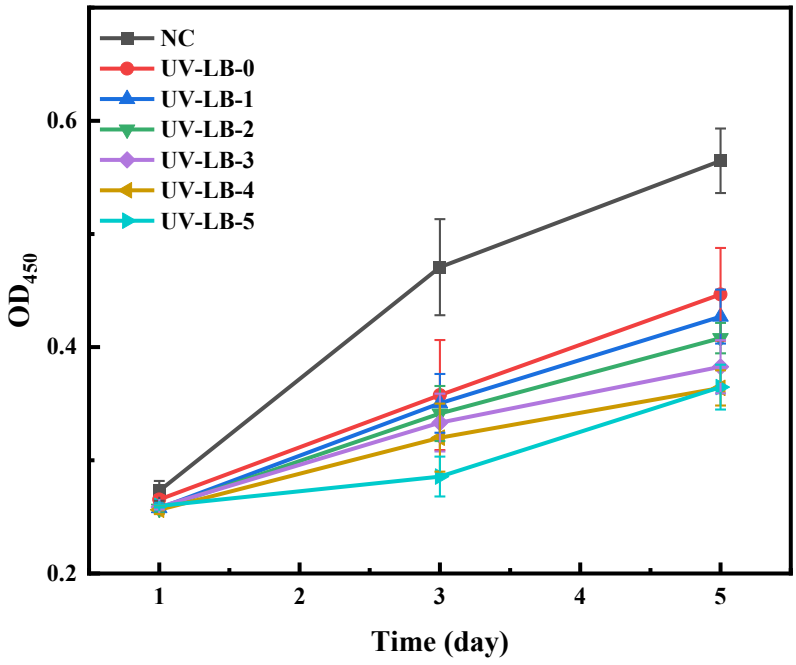

(a) OD_{450} value

 doi:10.20944/preprints202604.0115.v1

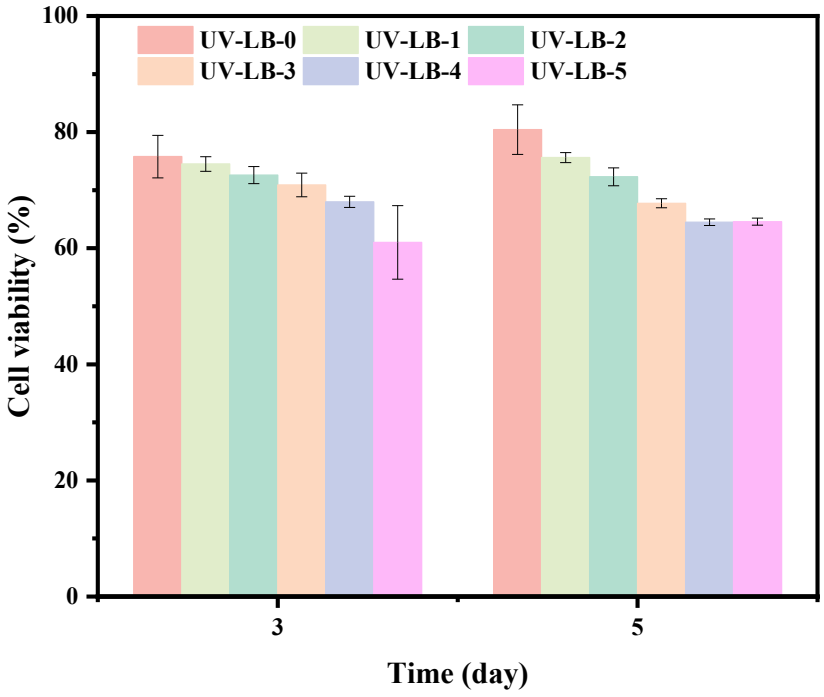

(b) Cell viability

Figure 5. Cytotoxicity study of UV−LBs against L929 cells.

3.7. Packaging Experiment of Resh−Cut Banana and Cherry Tomato

Fresh−cut fruits and vegetables are difficult to preserve due to the cutting process induced mechanical injury, which makes them susceptible to bacterial [7,8]. As depicted in Figure 6, the packaging investigation of fresh−cut cherry tomato and banana packaged by the UV−LBs was carried out. As demonstrated by Figure 6a, the CK of banana slice shows some black spots of spoilage at 6 h and it was spoiled obviously at 18 h. As to the fresh−cut banana slice packaged by UV−LB−10, though there were some spoiled black spots at 6 h, the content of spoilage was much less than that of CK. After packaged for 24 h, the fresh−cut banana slice packaged by UV−LB−10 begin to deteriorate obviously. When it comes to the fresh−cut banana slice packaged by UV−LB−25, the spoiled black spots occurred after packaged for 18 h and slightly deterioration occurred after packaged for 30 h. Clearly, when the fresh−cut banana slice packaged by UV−LB−30, there were almost no black deterioration spots occurred after packaged for 24 h. Even packaged by UV−LB−30 for 30 h, there is almost no sign of deterioration. So, it can be said that the storage time of fresh−cut banana packaged by UV−LB−30 can be extended from 12 h to 30 h.

As demonstrated by Figure 6b, the CK, the fresh−cut cherry tomatoes packaged by UV−LB−0 and UV−LB−10 showed obvious deterioration after 4 d, while the fresh−cut cherry tomatoes packaged by UV−LB−15, UV−LB−20 and UV−LB−25 begin to deteriorate obviously after packaged for 5 d. Clearly, the sample packaged by UV−LB−30 showed only slight deterioration after packaged for 5 d. It means that the the storage time of fresh−cut cherry tomato packaged by UV−LB−30 can be extended from 4 d to 5 d.

Overall, from the packaging experiment of both fresh−cut banana and cherry tomato above, it can be concluded that the storage time is extended with the increment of the amount of LB groups grafted on UV−LBs.

 doi:10.20944/preprints202604.0115.v1

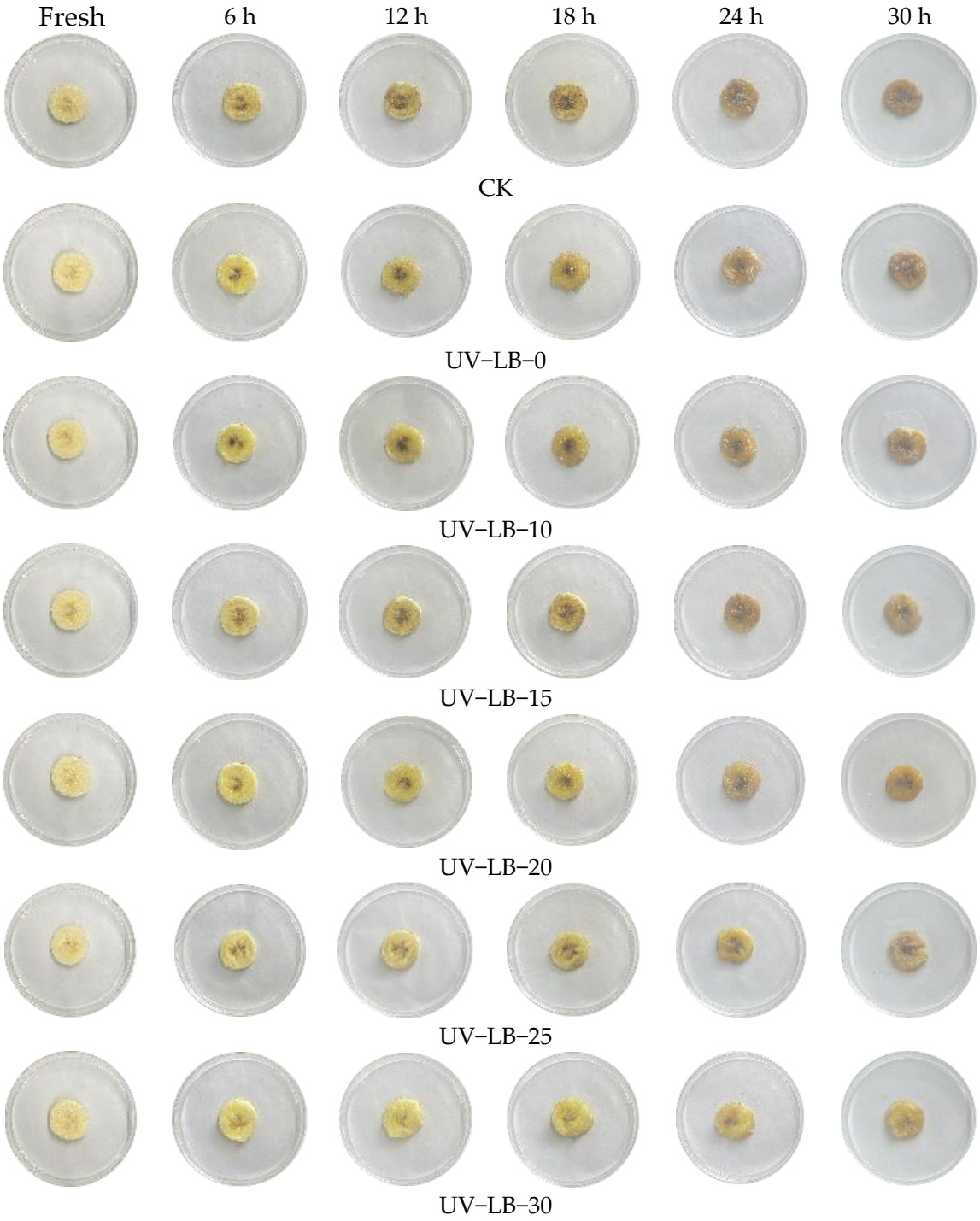

(a) Fresh−cut banana

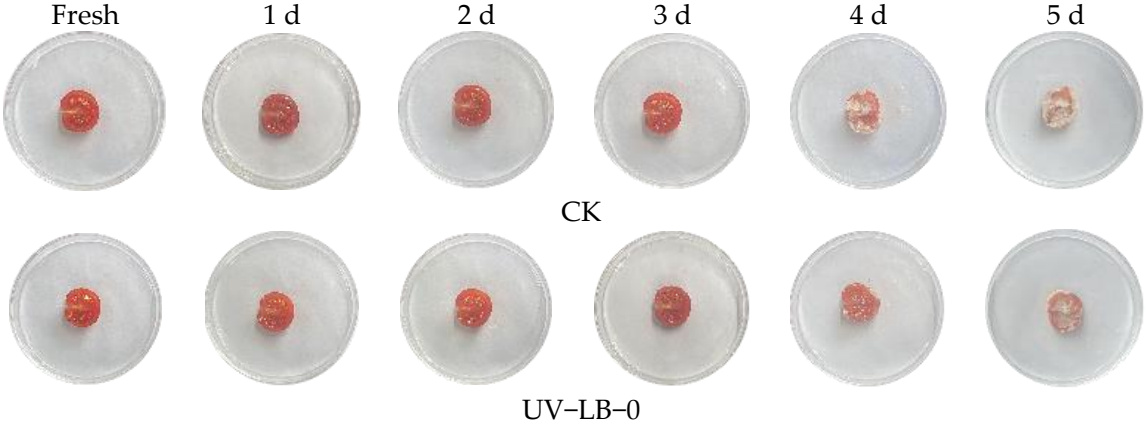

 doi:10.20944/preprints202604.0115.v1

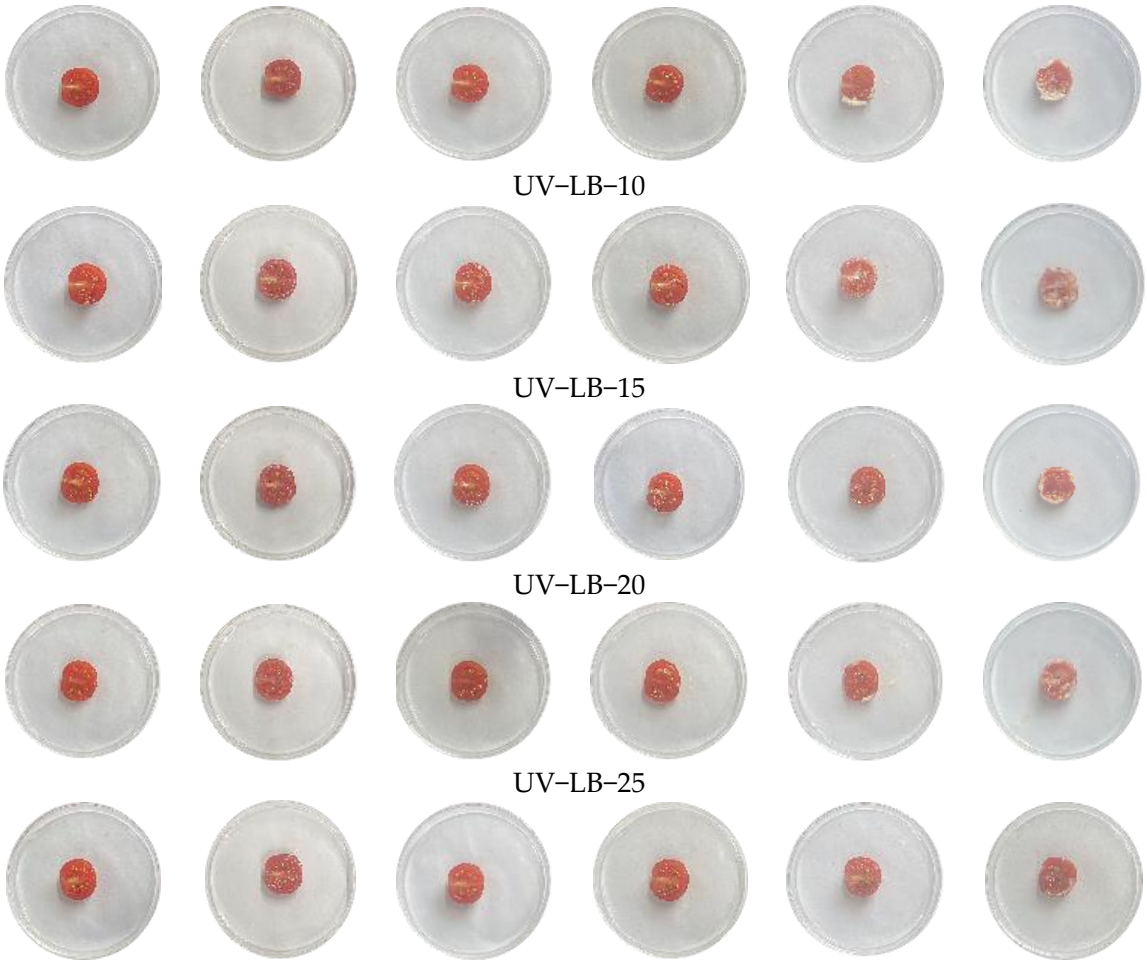

(b) Fresh−cut cherry tomato

Figure 6. Packaging investigation.

4. Conclusions

Antibacterial UV−curable antibacterial hydrogels were designed from LB−PUAs and PVA−SH through UV initiated thiol−ene click reaction. It revealed that T_{d5} of UV−LBs is in the range of 225−240 °C, which decreases with the increment of the molar ratio of L(-)−borneol to HPA from 30:70 to 0:100. DMA analysis shown the tensile strength and the elongation at break of UV−LBs are in the range of 1.38−2.05 MPa and 44.4−68.6%, respectively. When the molar ratio of L(-)−borneol to HPA is 15:85, the UV−LB−15 obtained reaches the highest tensile strength of 2.05 MPa by balancing the flexible units and the rigid units. A higher molar ratio of L(-)−borneol to HPA will achieve a higher antibacterial efficiency. The UV−LB−30 exhibited the highest antibacterial efficiency and it demonstrates antibacterial efficiency of 67.4% after 7 h against *S. aureus*, 75.6% after 8 h against *E. coli*, and 83.7% after 13 h against *M. albicans*. The storage time of fresh−cut banana and cherry tomato packaged by UV−LB−30 can be extended from 12 h to 30 h, 4 d to 5 d, respectively.

Supplementary Materials: The following supporting information can be downloaded at the website of this paper posted on Preprints.org, Figure S1: FT−IR spectra of PVA−SH and PVA. Figure S2: Procedure for fabrication LB−PUAs. Figure S3: FT−IR spectrum of LB−PUA−20. Figure S4: ^{1}H−NMR spectrum of LB−PUA−20. Figure S5. Scheme for fabrication UV−LBs. Figure S6. Scheme for the packaging investigation of fresh−cut banana and cherry tomato. Figure S7. FT−IR spectra of LB−PUA−30 and UV−LB−30. Figure S8. TGA curves of UV−LBs. Figure S9. Strain−stress curves of hydrogel films measured by DMA.

Author Contributions: Jizhong Yuan: Conceptualization, Methodology, Investigation, Data curation, Formal analysis, Writing−Original draft preparation. Yaohuang Jiang: Methodology, Investigation, Formal analysis.

 doi:10.20944/preprints202604.0115.v1

Mengle Liu: Investigation. Peipei Wu: Methodology. Guoxian Feng:Formal analysis. Yanchun Yu: Methodology and Supervision. Xiongfa Yang: Funding acquisition, Supervision, Conceptualization, Formal analysis, Writing Reviewing and Editing.

Acknowledgments: The authors highly appreciate the financial support from Yuyao Yuandong Chemical Co., Ltd. (L2024H00501).

Conflicts of Interest: The authors declare that they have no known competing financial interests or personal relationships that could have appeared to influence the work reported in this paper.

References

1. Han P., Sun J. Y., Mao S., Li F. Y., Yan X. X., Zhang T. H., Lu C. W. Multifunctional pectin−based films containing schiff base triggered by pH microenvironment for freshness monitoring and preservation of fresh−cut papayas, *Food Hydrocolloids*, 2024,157,110417.
2. Pan X. L., Duan Y., Liu S., Wang Y., Li Q., Jiang F. C., Li Y. X., Huang Z., Su L. J., Li X. B., Liu M. Y., Zhou X., Tang H. C. All−in−one: Harnessing multifunctional natural polysaccharide spray hydrogel loaded with polyphenol−metal nanoparticles for fruit preservation, *Food Chemistry*, 2025,470,142638.
3. Dwibedi V., Kaur G., George N., Rana P., Ge Y. H., Sun T. Research progress in the preservation and packaging of fruits and vegetables: From traditional methods to innovative technologies, *Food Packaging and Shelf Life,2024,*46, 101385.
4. Ganesh K. S., Sridhar A., Vishali S. Utilization of fruit and vegetable waste to produce value−added products: Conventional utilization and emerging opportunities A review. *Chemosphere,*2022,287,132221.
5. Han C. Q., Wang W. X., Suo B. X., Zhang J., Ma Q. Y., Sun J. F. Sodium nitroprusside affects energy metabolism, gamma−aminobutyric acid branching, and circRNA regulation of fresh−cut purple potatoes. *Postharvest Biology and Technology,2025,*227,113599.
6. Qiao L. P., Hou X. R., Li X. K., Hu N. J., Yang X., Wang Y. S., Li X. H., Lu L. F., Liu X. Glutamate induction of whole potatoes alleviated the browning of fresh cuts: Jasmonate signalling may play a key role, *Food Chemistry,*2025,482,144138.
7. Liu G. C., Liu R., Fu C. Y., Hu X., Li K., Yan L. K., Yang P., Zhao J. Protein/polysaccharide composite nanocoating based on amyloid−like aggregation for fresh−cut fruits preservation, *Chemical Engineering Journal,2025,*519,165048.
8. Liu L. L., Zhang Y. Y., Jin L. X., Abdollahi M., Zhao G. L., Venkatachalam K., Ban Z. J. Controlled release and stability enhancement of cinnamon essential oil in glutathione−modified soy protein particles: Its antimicrobial application for fresh−cut cantaloupe, *Food Research International,2025,*211, 116523.
9. Treviño−Garza M. Z., García S., Heredia N., Alanís−Guzmán M. G., Arévalo−Niño K. Layer−by−layer edible coatings based on mucilages, pullulan and chitosan and its effect on quality and preservation of fresh−cut pineapple (Ananas comosus), *Postharvest Biology and Technology*,2017,128, 63–75.
10. Alessio A., Eugenia G., Casales F. G., Gimenez M. J., Alessandra G., Gugino I. M., Daniela P., Giuseppe S. Extending shelf−life of fresh−cut apples using manna from ash tree (Fraxinus angustifolia) as natural antioxidant agent in comparision with calcium ascorbate, *Postharvest Biology and Technology*,2024,214,112986.
11. Wang D., Li D., Xu Y. Q., Li L., Belwal T., Zhang X. C., Luo Z. S. Elevated CO_2 alleviates browning development by modulating metabolisms of membrane lipids, proline, and GABA in fresh−cut Asian pear fruit, *Scientia Horticulturae*,2021,281,109932.
12. Sharma R., Nath P. C., Das P., Rustagi S., Sharma M., Sridhar N., Hazarika T. K., Rana P., Nayak P. K., Sridhar K. Essential oil−nanoemulsion based edible coating: Innovative sustainable preservation method for fresh/fresh−cut fruits and vegetables, *Food Chemistry*, 2024,460,140545.
13. Tsai P.−Y., Chen T.−Y., Chuang W.−T., Hsu S.−H. Self−assembled chitosan−boronic acid hydrogel as dynamic crosslinker to produce 3D−printable glucose−sensitive hydrogel, *Carbohydrate Polymers*,2025,363,123737.

 doi:10.20944/preprints202604.0115.v1

14. Wang X. J., Zhu H. Y., Yang Y. N., Lai G. Q., Yang X. F. UV−curable choline chloride and bromophenol red covalent functionalized chitosan antibacterial and pH−sensitive hydrogels, *Food Hydrocolloids*,2024,154,110103.
15. Wang X. J., Yuan J. Z., Sun N. N., Jiang Y. H., Yu Y. C., Lai G. Q., Yang X. F. UV−Curable antibacterial and pH−sensitive eugenol functionalized chitosan−polyurethane hydrogels for shelf−life extension of chicken, *Food Control,2025,* 168, 110918.
16. Mao L., Wang C. Y., Dong Z. Y., Yao J., Dong F., Dai X. L. Fabrication of polylactic acid bilayer composite films using polyvinyl alcohol based coatings containing functionalized carbon dots and layered clay for active food packaging, *Industrial Crops and Products*, 2025, 225,120460.
17. Wu J. J., Zhang Y., Zhang F.Y., Mi S., Yu W. L., Sang Y. X., Wang X. H. Preparation of chitosan/polyvinyl alcohol antibacterial indicator composite film loaded with AgNPs and purple sweet potato anthocyanins and its application in strawberry preservation, *Food Chemistry*,2025,463,141442.
18. Sheng W. Y., Yang L., Yang Y. C., Wang C. Z., Jiang G. Y., Tian Y. Q. Photo−responsive Cu−tannic acid nanoparticle−mediated antibacterial film for efficient preservation of strawberries, *Food Chemistry*,2025,464,141711.
19. Zhu Y. D., Pang X. H., Zhang W. L., Zhang C., Zhang B. L., Fu J. M., Zhao H. F., Han W. J. Green synthesis of silver nanoparticles using persimmon polysaccharides for enhanced polysaccharide−based film performance, *Food Research International*,2025,209,116252.
20. Wang Q., Zhang Z., Yin J., Shen L. Y., Zhu L. L., Redshaw C., Zhang Q. L. Block cationic copolymer/quaternary ammonium chitosan−based composite antibacterial hydrogel dressings with NIR photothermal effects for bacteria−infected wound healing, *International Journal of Biological Macromolecules*,2025,288,138716.
21. Cai Z. H., Wang L. Y., Zhang Q. Q., Yang W. Y., Zhang C., Wang H., Xiao H. M. Eco−friendly coating engineered with antimicrobial lipopeptides maintains freshness and induces genes expression in anthocyanin biosynthesis of blueberry, *International Journal of Biological Macromolecules*,2025,306,141590.
22. Li C. H., Zhao Y. X., Zhang A. J., Xu Y. C., Wang H. Y. Preparation, characterization, and antibacterial properties of a soybean protein isolate/gelatin composite film containing rosemary−modified bentonite and application of fresh lemon slices, *International Journal of Biological Macromolecules*,2025,308,142516.
23. Kumar B.T. S., Reddy J. P., Vanajakshi V., Dasalkar A. H., Yannam S. K., Hebbar U. H., Singh S. A. Development and characterization of carrageenan−based antibacterial films incorporated with natural melanin pigment from niger seed hulls (Guizotia abyssinica) and their efficacy to enhance the shelf−life of strawberries, *Food Control*,2025,174,111235.
24. Lu Z. W., Mu J. B., Guan C. W., Sui T. S., Liu C. Z., Guo Z. C., Liao S. M. Green and recyclable photocatalytic hydrogel film with antibacterial and ethylene scavenging properties for fruit preservation, *Food Chemistry*,2025,475,143266.
25. Yang H. J., Li L. P., Li C., Xu Z. H., Tao Y. H., Lu J., Xia X. D., Tan M. Q., Du J., Wang H. S. Multifunctional and antimicrobial carboxymethyl cellulose−based active hydrogel film for fruits packaging and preservation, *Food Bioscience,2024*,59,104005.
26. Yu K. J., Zhang S. Y., Yang L. N., Liu H., Li X. P., Xu Y. X., Li J. R. Strong, tough, antibacterial, antioxidant, biodegradable multi−functional intelligent hydrogel film for real−time detection and maintenance of salmon freshness, *Food Research International*, 2025,201,115594.
27. Gong W., Yang T. Q., He W. Y., Li Y. X., Hu J. N. On−demand removable hydrogel film derived from gallic acid−phycocyanin and polyvinyl alcohol for fruit preservation, *Food Chemistry*,2025,463,141404.
28. Wu Y. B., Gu Z. M., Chen T. T., Zu D. T., Gan Y. H., Chen H. L., Yang J. N., Yu X., Cai H. H., Sun P. H., Ning J. Y., Zhou H. B., Zheng J. X. Effect of different crosslinking agents on carboxymethyl chitosan−glycyrrhizic acid hydrogel: Characterization and biological activities comparison, *International Journal of Biological Macromolecules*,2025,298, 139977.
29. Qian Y., Zheng Y., Jin J., Wu X., Xu K., Dai M., Niu Q., Zheng H., He X., Shen J. Immunoregulation in diabetic wound repair with a photoenhanced glycyrrhizic acid hydrogel scaffold, *Advanced Materials*,2022,34 (29),2200521.

 doi:10.20944/preprints202604.0115.v1

30. Laquerbe S., Sayed J. E., Lorthioir C., Meyer C., Narita T., Ducouret G., Perrin P., Sanson N. Supramolecular crosslinked hydrogels: similarities and differences with chemically crosslinked hydrogels, *Macromolecules*,2023,56(18),7406–7418.
31. Mehta P., Sharma M., Devi M.. Hydrogels: an overview of its classifications, properties, and applications, *Journal of the Mechanical Behavior of Biomedical Materials*,2023,147,106145.
32. Wang D. B., Zhu C. Q., Yang Q. F., Xu Y. Q., Zhang D. Q., Wang D. Y., Liu F., Hou C. L. Stretchable, controlled release of active substances, and biodegradable chitosan−polyvinyl alcohol hydrogel film for antibacterial and chilled meat preservation, *Food Chemistry*, 2025, 477,143608.
33. Sanchez−Cid P., Alonso−Gonzalez M., Jimenez−Rosado M., Benhnia M. R. E., RuizMateos E., Ostos F. J., Romero A., Perez−Puyana V. M. Effect of different crosslinking agents on hybrid chitosan/collagen hydrogels for potential tissue engineering applications, *International Journal of Biological Macromolecules*,2024,263,129858.
34. Dodda J. M., Azar M. G., Sadiku R. Crosslinking trends in multicomponent hydrogels for biomedical applications, *Macromolecular Bioscience*,2021,21 (12), 2100232.
35. Lechuga−Islas V. D., Gillissen E., Bourguignon M., Grignard B., Detrembleur C. Foam−to−adhesive recycling of self−blown non−isocyanate polyurethane foams facilitated by integration of disulfide exchangeable bonds and moisture, *Chemical Engineering Journal*, 2025,516,163998.
36. Wang W., Coenye T., Su J. Y., Qiu S.−X. Biofilm inhibition and eradication activity of citral and borneol against foodborne bacteria, *Industrial Crops and Products*,2025,223,120199.
37. Zhou Z. L., Chen R. X., Li P. Z., Fan P. H., Ma L., Cai X. Y., Hou Y. C., Li B. B., Su J. Y. Natural borneol improves cellular uptake of curcumin to enhance its photodynamic bactericidal activity against Escherichia coli ATCC 8739, *Food Microbiology*,2025,127, 104686.
38. Zhao Z. J., Fan X., Li X. Y., Qiu Y. W., Yi Y. F., Wei Y. P., Wang Y. All−natural injectable antibacterial hydrogel enabled by chitosan and borneol, *Biomacromolecules*,2024,25, 134−142.
39. Gao X., Zhang H. C., Yan C. F., Wu J., Wang Y. T., Jiang M. H., Wang Y. N. Yunnan Baiyao−enhanced cellulose nanofiber composite hydrogel wearable patch for transdermal drug delivery and anti−freezing applications, *International Journal of Biological Macromolecules*,2025,315,144684.
40. Deng Z. X., Guo Y., Wang X. F., Song J. J., Yang G., Shen L. T., Wang Y. H., Zhao X., Guo B. L., Wang W. Multiple crosslinked, self−healing, and shape−adaptable hydrogel laden with pain−relieving chitosan@borneol nanoparticles for infected burn wound healing, *Theranostics*,2025,15(4):1439−1455.
41. Liu Z. Z., Liao H. B., Li H. L., Zou Z. R. Fabrication and characterization of cinnamomum camphora chvar. Borneol essential oil microcapsules decorated by β−cyclodextrin with ultrasound−assisted complexation method, *Arabian Journal for Science and Engineering*. 2025,50(24):20599−20612.
42. Abbasi Z., Esfandiari Z., Rostamabadi H. Postbiotic−loaded κ−carrageenan hydrogels double cross−linked with carboxymethyl cellulose and calcium ions, *Food Hydrocolloids*,2025,168, 111551.
43. Yang Z. M., Liu Y., Wang E. Z., Yin W., Wang Y. J., Guo Y. C., Zhang W. T., Qi H. Insights into the highly selective and efficient adsorption of Pb^{2+} by fish skin collagen−enabled sodium alginate−based composite gel spheres: adsorption and interference mechanisms, *Food Hydrocolloids*,2026,170,111700.
44. Feng X., Li M., Li S. H., Lin M. T., Nie Y., Yao N., Deng T. X., Yang X. H., Ding H. Y., Xu L. N. Fabrication and properties of recyclable tung oil–based polymer coatings based on dual cross–linked dynamic covalent polymer networks, *Progress in Organic Coatings*,2024,192, 108521.
45. Kim G. Y., Sung S. J., Kim M. P., Kim S. C., Lee S. H., Park Y. I., Noh S. M., Cheong I. W., Kim J. C. Reversible polymer networks based on the dynamic hindered urea bond for scratch healing in automotive clearcoats, *Applied Surface Science*,2020,505,144546.
46. Liu W. Z., Li L., Liu S. N., Liu B., Wu Z. Y., Deng J. R. Novel robust ion−specific responsive photonic hydrogel elastomer, *Journal of Materials Chemistry C*,2024,7(29):8946−8953.